Escola de Primavera de Transição e Turbulência
Blumenau 2022

ABCM
13th Spring School on Transition and Turbulence
September 19th-23rd, 2022, Blumenau, SC, Brazil

EPTT-2022-0019
ASSESSMENT OF A NEW HYBRID TURBULENCE MODEL APPLIED TO CYCLONE SEPARATORS

Rafaela Gomide Corrêa
Francisco José de Souza
Fluid Mechanics Laboratory, Federal University of Uberlândia
Av. João Naves de Ávila, 2121, Bloco 5P - 38408-014 - Uberlândia - Minas Gerais - Brasil
rafaelagomide@ufu.br
francisco.souza@ufu.br

Abstract. *Cyclones are devices that use the centrifugal acceleration to separate particles from a gas flow. The models as the current ones started to show up in the beginning of the twentieth century and their development was promoted by their simple construction, low manufacturing cost, lack of moving parts and relative ease of maintenance. The flow inside a cyclone, formed by the tangential feed under high pressure, is turbulent, multiphasic and complex. This flow is responsible for the separation, so it has been widely studied to understand and optimize the operation of this equipment. To analyze a fluid flow, one alternative is to solve the equations of continuity, momentum and energy. When there are particles in the flow, it is also necessary to solve equations for their motion, generating an equations system that is hard to solve analytically. Then it is required to use Computational Fluid Dynamics (CFD) and, to obtain a result that is similar to the reality, the turbulence model needs to be appropriate. For cyclones, the most used models are the Large Eddy Simulation (LES) and the Reynolds Stress Model (RSM). The first one can give more accurate results, but it needs a more refined mesh and has higher computational costs. So, to combine the advantages of these two models, the main objective of this research was to evaluate a new hybrid LES/RSM model applied to the cyclone's flow. The results were compared to experimental data and with RSM model results. It showed that the grade collection efficiency curve obtained by the hybrid model is closer to the experimental one, even for the less refined mesh. Furthermore, the velocity field obtained by the two models were compared and the results were similar, but the hybrid model predicts more fluctuations. It suggests that resolving some of the length scales is important to the grade collection efficiency.*

Keywords: *Cyclone, Hybrid LES/RSM, Large Eddy Simulation (LES), Reynolds Stress Model (RSM), Collection efficiency*

1. INTRODUCTION

Cyclones are devices that separate particles from a gas flow using the centrifugal acceleration. The first cyclone model appeared in 1885, but several changes were made to reach the current models. There are still many studies to optimize these devices for specific applications, since its efficiency is linked to the geometry and functionment conditions. The cyclone researches are also made because it is used in several industries, like oil, grain, food and mining (Hoffmann and Stein, 2008).

It is important to analyze the flow that occurs inside the cyclones, since its behavior directly affects the equipment efficiency, due to the active separation mechanism. As the majority of the flows in the industry, the cyclone flow is complex and turbulent, points that make its analysis difficult. But with the computational advance and using high-performance computers, it became possible to predict such flows by using Computational Fluid Dynamics.

Even with modern numerical techniques, it is difficult to solve turbulent flows, mostly because they have several turbulent scales and as higher is the Reynolds number of a flow, higher is the number of turbulent scales and the number of equations in the equations system that must be solved in the flow analysis. Even with all the advancement that has already hapened, it is still not possible to solve all the degrees of freedom that represent a complex flow, so it is necessary to model some (Silveira Neto, 2001).

In turbulence modelling there are two main methodologies: the RANS and the LES. In the Reynolds Average Navier-Stokes (RANS) equations, the turbulent scales are devided in mean behavior and fluctuations, causing all the scales to be modeled.In Large Eddy Simulation (LES), the Navier-Stokes equations are filtered in space, separating the scales in large and subgrid scales, modelling the small ones and solving the large ones (Silveira Neto, 2001). It is an advantage to model only a small part of the flow, but it requires more refined meshes and has a higher computational cost. To combine the advantages of these two methodologies, the hybrid models were created. They use the RANS equations in some regions of the domain and LES in others, to obtain more realistic results with lower computational costs.

In order to obtain meaningful results in numerical simulations with computational cost consistent with the current capabilities, the present paper aimed to propose and evaluate a hybrid LES-RSM model applied to cyclone flow. The simulations were performed with three diferents inlet flow rates. Fluid flow variables were compared with the results obtaines with the Reynolds Stress Model (RSM) and the influence of the velocity fluctuations was analyzed. Futhermore, experimental data of collection efficiency were used to compare the accuracy of the hybrid model with the RSM model.

2. METHODOLOGY

2.1 Geometry and grids

To validate the hybrid model proposed in the present paper and to compare it with the RSM results, experimental data from Xiang *et al.* (2001) were used. The geometry is presented in the Fig. 1 and the dimensios are shown in the Tab. 1.

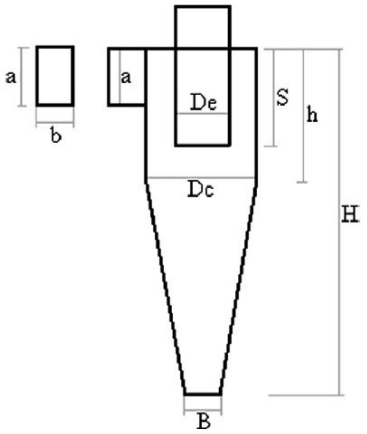

Figure 1: Cyclone geometry. Adapted from Xiang *et al.* (2001).

Table 1: Cyclone dimensions (Xiang *et al.*, 2001)

Dimension	Length (mm)
Body diameter (Dc)	31
Gas outlet diameter (De)	15.5
Inlet height (a)	12.5
Inlet width (b)	5
Cyclone height (H)	77
Cylinder height (h)	31
Gas outlet duct length (S)	15.5
Cone bottom opening (B)	19.4

The physical model is an incompressible flow, with constant physical properties, newtonian fluid and without thermal effects. The fluid phase is air, with density equal to 1.205 kg/m³ and viscosity equal to 1.82 $\times 10^{-5}$ kg/m.s. The inlet velocities used were 8 m/s, 10.67 m/s and 13.33 m/s, which leads to Reynolds numbers of 16420, 21900 and 27360, respectively, which characterizes turbulent flows.

For the disperse phase, particles with a density of 1050 kg/m³ injected at the same velocity as the fluid and with mass flow rate equal to 0.000275 kg/s were used. 96000 particles were injected in the first time step, 8000 of each diameter varying between 0.5 μm and 6 μm. It was considered that the particles reflected when colliding with the wall, escaped when crossing the overflow and were collected when touching the underflow.

To solve the problem, three meshes, with nearly 180 000, 400 000 and 800 000 hexaedra, were used.

2.2 Mathematical model

In this paper, two diferents mathematical models were used for the fluid phase: the RSM and the hybrid model. These two models and the model used for the dispersed phase will be shown in this section.

The numerical solution of the equations that will be presented is made using the computational code UNSCYFL3D. This in-house software is based on the finite volume method in unstructured three-dimensional grids. In all the simulations carried out in this work the three-time-level scheme was used for time-advancement, the centered differencing scheme was employed for the diffusive term of the momentum equations and the second order upwind scheme was used for the advective term of the momentum equations. The SIMPLE (Semi-Implicit Method for Pressure-Linked Equations) algorithm is used to couple the velocity and pressure fields.

2.2.1 RSM model

In the Reynols Stress Model, the equations for each component of Reynolds stress are obtained by filtering the Navier-Stokes equations, leading to

$$\begin{aligned}\frac{\partial(\rho\overline{u_i{'}u_j{'}})}{\partial t} = &-\frac{\partial(\rho\overline{u_k{'}u_i{'}u_j{'}})}{\partial x_k} - \frac{\partial}{\partial x_k}\left[\rho\overline{u_i{'}u_j{'}u_k{'}} + \overline{p\left(\delta_{kj}u_i' + \delta_{ik}u_j'\right)}\right] + \frac{\partial}{\partial x_k}\left[\mu\left(\frac{\partial\overline{u_i{'}u_j{'}}}{\partial x_k}\right)\right] \\ &-\rho\left(\overline{u_i{'}u_k{'}}\frac{\partial\overline{u_j}}{\partial x_k} + \overline{u_j{'}u_k{'}}\frac{\partial\overline{u_i}}{\partial x_k}\right) + \overline{p\left(\frac{\partial u_i'}{\partial x_j} + \frac{\partial u_j'}{\partial x_i}\right)} - 2\mu\overline{\frac{\partial u_i'}{\partial x_k}\frac{\partial u_j'}{\partial x_k}}\end{aligned} \tag{1}$$

$\overline{u_i{'}u_j{'}}$ is the Reynolds stress, ρ is the density, p is the pressure, δ is the Kronecker tensor, μ is the viscosity, u_i are the velocity components and x_i are the position components. Some terms in the Eq. 1 need to be modeled, leading to

$$\begin{aligned}\frac{\partial(\rho\overline{u_i{'}u_j{'}})}{\partial t} = &-\frac{\partial(\rho\overline{u_k{'}u_i{'}u_j{'}})}{\partial x_k} - \frac{\partial}{\partial x_k}\left[\frac{\mu_t}{\sigma_k}\left(\frac{\partial\overline{u_i'u_j'}}{\partial x_k}\right)\right] + \frac{\partial}{\partial x_k}\left[\mu\left(\frac{\partial\overline{u_i{'}u_j{'}}}{\partial x_k}\right)\right] \\ &-\rho\left(\overline{u_i{'}u_k{'}}\frac{\partial\overline{u_j}}{\partial x_k} + \overline{u_j{'}u_k{'}}\frac{\partial\overline{u_i}}{\partial x_k}\right) + \phi_{ij,1} + \phi_{ij,2} + \phi_{ij,3} - \varepsilon\end{aligned} \tag{2}$$

Where

$$\phi_{ij,1} = -C_1\frac{\varepsilon}{k}\left(\overline{u_i'u_j'} - \frac{2}{3}\delta_{ij}k\right) \tag{3}$$

$$\phi_{ij,2} = -C_2\left[(P_{ij} - A_{ij}) - \frac{2}{3}\delta_{ij}P_{ij}\right] \tag{4}$$

$$\begin{aligned}\phi_{ij,3} = &C_{1,w}\frac{\varepsilon}{k}\left(\overline{u_k'u_m'}n_kn_m\delta_{ij} - \frac{3}{2}\overline{u_i'u_k'}n_jn_k - \frac{3}{2}\overline{u_j'u_k'}n_in_k\right)\frac{k^{\frac{3}{2}}}{C_l\varepsilon d} \\ &+C_{2,w}\left(\phi_{km,2}n_kn_m\delta_{ij} - \frac{3}{2}\phi_{ik,2}n_jn_k - \frac{3}{2}\phi_{jk,2}n_in_k\right)\frac{k^{\frac{3}{2}}}{C_l\varepsilon d}\end{aligned} \tag{5}$$

$$\frac{\partial(\rho\varepsilon)}{\partial t} + \frac{\partial(\rho\varepsilon u_i)}{\partial x_i} = \frac{\partial}{\partial x_j}\left[\left(\mu + \frac{\mu_t}{\sigma_\varepsilon}\right)\frac{\partial k}{\partial x_j}\right] + \frac{C_{\varepsilon1}\varepsilon P_{ii}}{2k} - \frac{C_{\varepsilon2}\rho\varepsilon^2}{k} \tag{6}$$

ε is the turbulent dissipation, k is the turbulent kinetic energy, P_{ij} is the transformation term, A_{ij} is the advective term, n_k is the vector unit normal to the wall x_k and d is the distance to the wall. $C_1, C_2, C_{1,w}$ e $C_{2,w}$ are empirical constants and C_l is equal to 0.39. $C_{\varepsilon1}$ and $C_{\varepsilon2}$ are equal to 1.2, σ_k is 0.82 and σ_ε is 1.

2.2.2 Hybrid LES-RSM model

The hybrid model proposed for the current paper is based on the work of Hadžiabdic and Hanjalic (2020). It uses a grid detecting parameter α thet is inserted in the RSM equations following the turbulent dissipation. It makes the dissipation decrease where the mesh is sufficiently refined and more turbulent scales are solved. The equations are

$$\begin{aligned}\frac{\partial(\rho\overline{u_i{'}u_j{'}})}{\partial t} = &-\frac{\partial(\rho\overline{u_k{'}u_i{'}u_j{'}})}{\partial x_k} - \frac{\partial}{\partial x_k}\left[\frac{\mu_t}{\sigma_k}\left(\frac{\partial\overline{u_i'u_j'}}{\partial x_k}\right)\right] + \frac{\partial}{\partial x_k}\left[\mu\left(\frac{\partial\overline{u_i{'}u_j{'}}}{\partial x_k}\right)\right] \\ &-\rho\left(\overline{u_i{'}u_k{'}}\frac{\partial\overline{u_j}}{\partial x_k} + \overline{u_j{'}u_k{'}}\frac{\partial\overline{u_i}}{\partial x_k}\right) + \phi_{ij,1} + \phi_{ij,2} + \phi_{ij,3} - \alpha\varepsilon\end{aligned} \tag{7}$$

$$\phi_{ij,1} = -C_1\frac{\alpha\varepsilon}{k}\left(\overline{u_i'u_j'} - \frac{2}{3}\delta_{ij}k\right) \tag{8}$$

$$\phi_{ij,2} = -C_2 \left[(P_{ij} - A_{ij}) - \frac{2}{3}\delta_{ij} P_{ij} \right] \tag{9}$$

$$\begin{aligned} \phi_{ij,3} = C_{1,w} \frac{\alpha\varepsilon}{k} \left(\overline{u'_k u'_m} n_k n_m \delta_{ij} - \frac{3}{2}\overline{u'_i u'_k} n_j n_k - \frac{3}{2}\overline{u'_j u'_k} n_i n_k \right) \frac{k^{\frac{3}{2}}}{C_l \alpha \varepsilon d} \\ + C_{2,w} \left(\phi_{km,2} n_k n_m \delta_{ij} - \frac{3}{2}\phi_{ik,2} n_j n_k - \frac{3}{2}\phi_{jk,2} n_i n_k \right) \frac{k^{\frac{3}{2}}}{C_l \alpha \varepsilon d} \end{aligned} \tag{10}$$

The grid detecting parameter is obtained from

$$\alpha = max \left(1, \frac{L_{RANS}}{L_{LES}} \right) \tag{11}$$

where

$$L_{RANS} = \frac{k^{1.5}}{\varepsilon} \tag{12}$$

$$L_{LES} = C_\Delta (\Delta V)^{1/3} \tag{13}$$

k is the modeled turbulent kinetic energy and C_Δ is a constant. The equation for the turbulent dissipation remains Eq. 6.

To act like a hybrid model with LES in outer flow region, the funtion α changes the implicit characteristic turbulence length scale from the RANS, L_{RANS}, to the subgrid scale from LES when it becomes smaller than L_{RANS}. The model also uses a switching model criterion that selects the turbulent viscosity between the two models.

$$\nu_t = max(\nu_t^{RANS}, \nu_t^{LES}) \tag{14}$$

Then, close to the wall $\alpha = 1$ and the model acts like URANS. Away from the wall, $L_{RANS} > L_{LES}$ and $\alpha > 1$, which decrases ν_t^{RANS}.

As α begame greater than 1, the solved energy increases. Thus, to calculate L_{RANS} the total turbulent kinect energy (k_{tot}) must be considered. It is obtained by adding of the solved part (k_{res}) and the modeled part (k_{mod}). The Eq. 12 is rewritten as

$$L_{RANS} = \frac{k_{tot}^{1.5}}{\varepsilon} = \frac{(k_{res} + k_{mod})^{1.5}}{\varepsilon} \tag{15}$$

2.2.3 Dispersed phase modeling

The dispersed phase is treated in a Lagrangian framework, so each particle is tracked trough the domain and its motion is described based on the Newton's second law.

$$\frac{dx_{pi}}{dt} = u_{pi} \tag{16}$$

$$m_p \frac{du_{pi}}{dt} = m_p \frac{3\rho C_D}{4\rho_p d_p}(u_i - u_{pi}) + \left(1 - \frac{\rho}{\rho_p}\right) m_p g_i \tag{17}$$

$$I_p \frac{d\omega_{pi}}{dt} = T_i \tag{18}$$

d_p is the particle diameter, m_p is the particle mass and I_p is the moment of inertia for an espherical particle. To calculate the drag coefficient (C_D) the correlation of Shiller and Naumann (1935) is used.

$$C_D = \begin{cases} 24Re_p^{-1}\left(1 + 0.15Re_p^{0.687}\right) \text{ if } Re_p < 1000 \\ 0.44 \text{ if } Re_p > 1000 \end{cases} \tag{19}$$

$$Re_p = \frac{\rho d_p |\overrightarrow{u} - \overrightarrow{u}_p|}{\mu} \tag{20}$$

One last equation is needed to calculate the torque (T_i) that appears in Eq. 18.

$$\overrightarrow{T} = C_r \frac{\rho d_p^5}{64} |\overrightarrow{\Omega}| \overrightarrow{\Omega} \tag{21}$$

$$C_r = \begin{cases} \frac{64\pi}{Re_r} \text{ if } Re_r < 32 \\ \frac{12.9}{\sqrt{Re_r}} + \frac{128.4}{Re_r} \text{ if } Re_r > 32 \end{cases} \tag{22}$$

In Eq. 17 forces such as Saffman's, Basset and virtual force have been neglected. This can be done in the current case, because the particle material density is nearly 1000 times the gas density (Salvo, 2009; Santos, 2019).

3. RESULTS AND DISCUSSIONS

3.1 Velocity profile

As the Reynolds number for the three inlet flow rates are close, the analysis for the velocity profile will be done only for the intermediate value and its behavior can be extended for the other two flow rates. The velocity profile was obtained at a line positioned at 0.05 m in a section in the X plane located in the center of the cyclone.

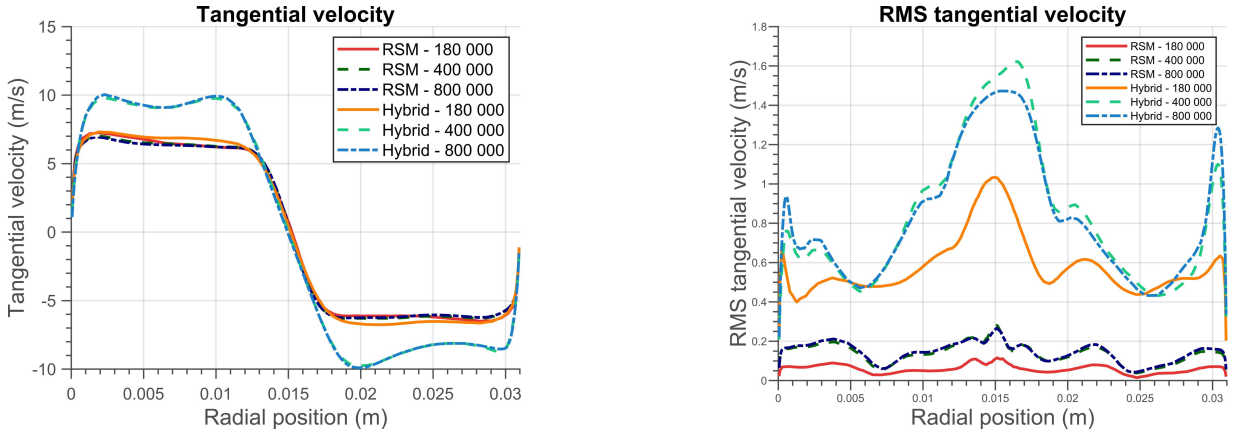

(a) (b)

Figure 2: Velocity profile for the flow rate of 40 l/min (a) mean tangential velocity and (b) RMS tangential velocity

Figure 2a shows the tangencial velocity profile for the three different grids and the two different models used in the present paper. It can be observed that in all cases the tangencial velocity profile presents positive values on the left side and negative values on the right side, indicating the rotational movement around the central axis, as expected.

Comparing the two models in the same mesh, it can be seen that in the grid with 180 000 volumes the results of the two models were similar. But in the 400 000 and 800 000 grids the difference between the maximum and minimum values obtained with the two different models is greater. This is explained by the fact that the coarser grid is not refined enough to allow the hybrid model to use the LES model in much of the domain, so the hybrid model works almost like the RSM.

Comparing the three meshes in the same model, it is noted that for the RSM model the results for the three grids were very close, but for the hybrid model only the meshes with 400 000 and 800 000 volumes were close, while the 180 000 grid obtained a lower result. This indicates that for the RSM model the grid independence was achieved, so increasing the refinement does not generate important differences in the results. For the hybrid model the coarser mesh does not allow the hybrid model to use the LES model in much of the domain, while the two more refined meshes allow it, generating a great difference between the results.

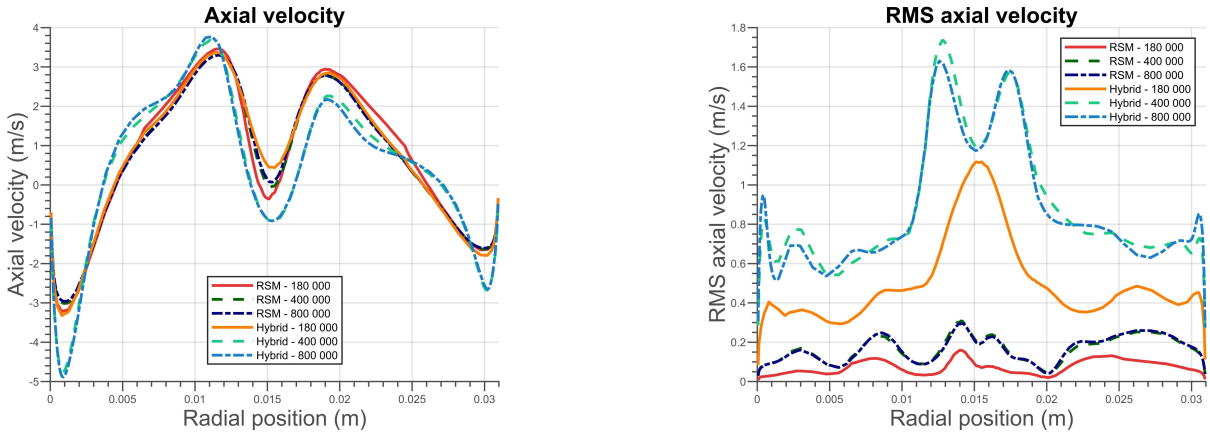

(a) (b)

Figure 3: Velocity profile for the flow rate of 40 l/min (a) mean axial velocity and (b) RMS axial velocity

Another important point to be analyzed is the RMS velocity, that represents the fluctuation of the velocity. Figure 2b shows that the hybrid model generated higher values of RMS velocity than the RSM model, which was expected, since the RSM model models the mean velocity while the hybrid model uses the LES in some regions, calculating the instantaneous velocity.

A similar analysis can be made for the axial component of velocity. Figure 3a shows that negative values of velocity were obtained near the walls and approaching the center, the values increased, becomig positives. This inverted W profile was expected. The behavior of the six cases was the same observed in the tangential velocity. For the RSM the three meshes generated very close results and for the hybrid model the coarser mesh generated results far from the ones of the two other meshes. Futhermore, the hybrid model results were distant from the RSM for the grids of 400 000 and 800 000 volumes, while the mesh of 180 000 hexaedra generated similar results in both models.

3.2 Turbulent kinetic energy

The turbulent kinetic energy decomposed in modeled and solved parts is important to show the concept of the used models. The analysis was performed for the 800 000 volumes grid, since for a finer mesh the hybrid model tends to use the LES in more parts of the domain, making the difference with the RSM model more evident. The contour of the turbulent kinetic energy was obtained in the same plane as the velocity profile.

It is known that the hybrid model uses the LES model in some parts of the domain, which solves the equations for the large scales and models the subgrid scales. Beyond that, the RSM model is characterized for modeling almost all turbulent scales. This behavior is shown in Figs. 4 and 5. In the hybrid model, the modeled portion only has high values near the wall, where the RSM is used. In the outer flow region, the modeled portion is close to zero, proving that only a few scales are modeled, and the solved part has high values, showing that most scales are solved. For the RSM model the modeled part is high in the whole domain and the solved part is non-zero only in a small part at the gas outlet duct, proving that this model models almost all turbulent scales.

3.3 Collection efficiency

The collection efficiency shows the influence of the models and grids in the calculation of the particle motion. To analyze this variable, experimental data from Xiang *et al.* (2001) were used and plotted with the numerical results of the current paper. To determine which particles were collected, the underflow was defined as wall and all particles that touched this wall were considered collected.

Figures 6, 7 and 8 show that all cases generated S shaped collection efficiency curves, which is in agreement with the theory.

Analysing the differences between the models, it is noticed that the hybrid model generated collection efficiency values closer to the experimental ones. For small particles the RSM model obtained values much higher than the experimental data and for the medium and big particles, it generated values much lower than those of the experiments. The proximity with the experimental data happens because the hybrid model uses LES in some parts of the domain, calculating more turbulent scales than the RSM model. Decrease the modeled part tends to yield more realistics results, as observed. Futhermore, as showed in the velocity profiles, the hybrid model obtained higher values of velocity, which generates greater centrifugal force on the particles. This causes more particles to be carried to the wall and consequently to the underflow, increasing the collection efficiency. On the other hand, as shown by Souza *et al.* (2012), a higher velocity

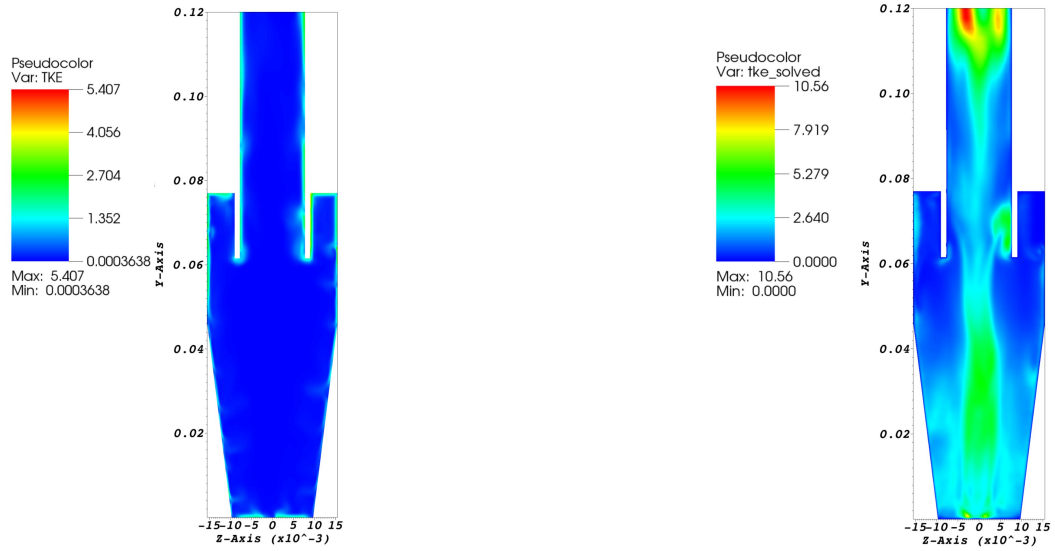

(a) (b)

Figure 4: Turbulent kinetic energy for the flow rate of 40 l/min, 800 000 grid and hybrid model (a) modeled and (b) solved

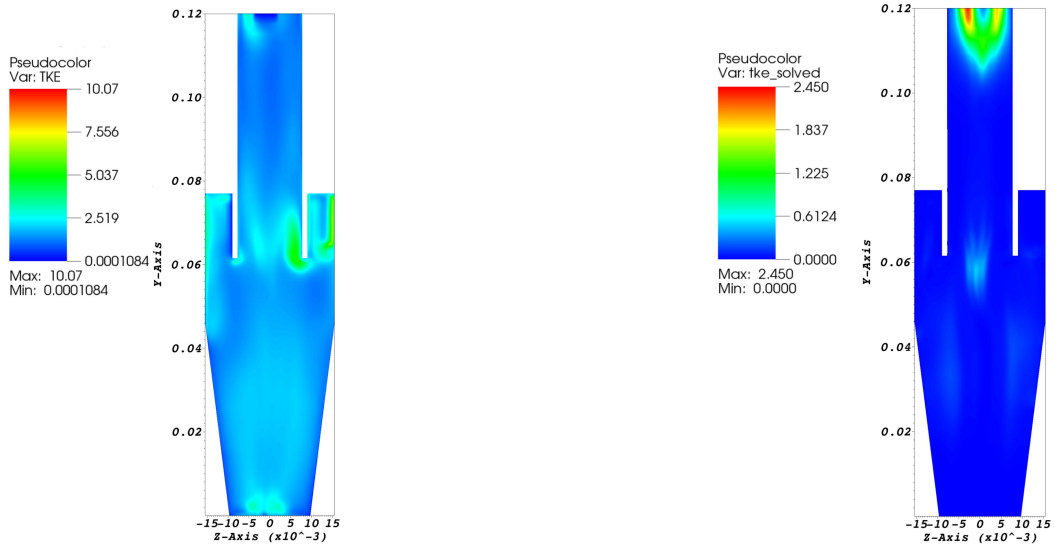

(a) (b)

Figure 5: Turbulent kinetic energy for the flow rate of 40 l/min, 800 000 grid and RSM model (a) modeled and (b) solved

increases the turbulence which causes the reentrainment of particles that would be otherwise collected and consequently disturbs the separation efficiency. In the studied cases the combination of these factors caused an increase in the collection efficiency calculated by the hybrid model compared to the RSM. For small particles the decrease on the collection efficiency, getting closer to the experimental data, is caused by the velocity fluctuations. As shown in the velocity profiles, the hybrid model generated higher values for RMS velocity, since it calculates the instantaneous velocity and the RSM calculate the mean velocities. These fluctuations are important to the particles motion, especially for the small ones that follow the changes in the flow more easily. This result is in agreement with Shukla *et al.* (2013).

Analysing the influence of the used grids, it is noticed that for the flow rate of 30 l/min the values obtained for the three meshes with the RSM model were very close, especially for diameters greater than 4 μm. For the hybrid model, the results for the 180 000 volumes grid were distant of those obtained by the 400 000 and 800 000 meshes, which were very close to each other and to the experimental data. This behavior reflects what was observed in the velocities, where the values obtained by the two more refined meshes were close to each other and far from the coarser mesh result. The proximity with the experimental data happens because the hybrid model calculates more turbulent scales, making the results closer to the reality, as expected. For the flow rates of 40 l/min and 50 l/min, there is a greater difference between the results of

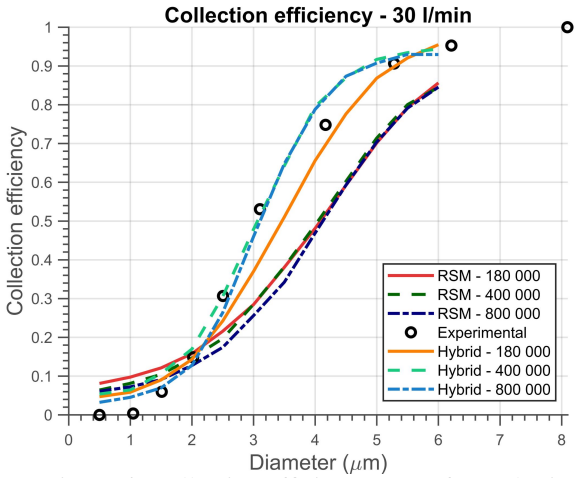

Figure 6: Collection efficiency curve for 30 l/min

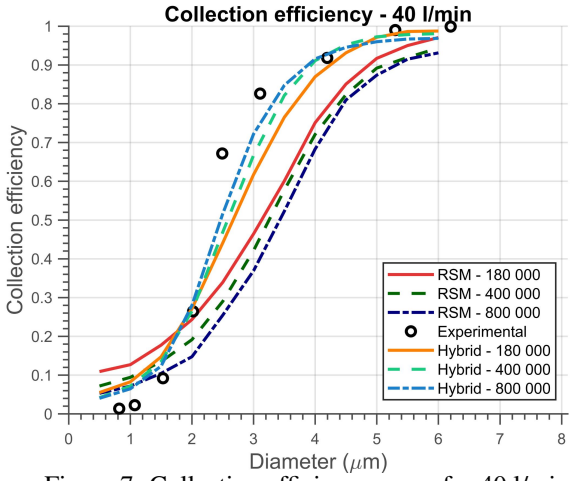

Figure 7: Collection efficiency curve for 40 l/min

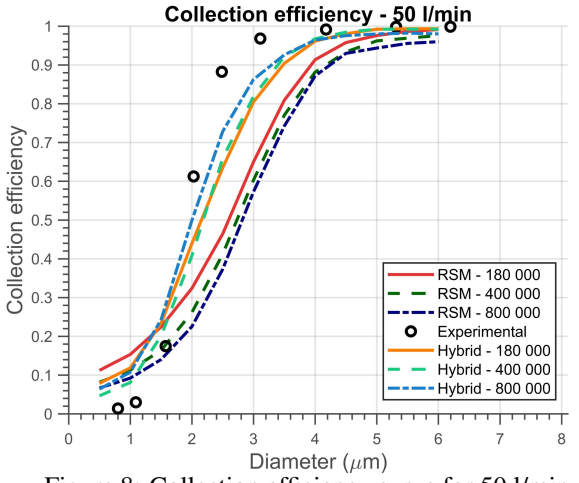

Figure 8: Collection efficiency curve for 50 l/min

the RSM model with the three meshes. This indicates that the small differences observed in the fluid flow were sufficient to change the particles motion. For the hybrid model, it can be noticed that the values obtained for the meshes of 800 000 and 400 000 volumes are more distant from each other and the results of 400 000 and 180 000 volumes grids are closer to each other, compared to 30 l/min. Futhermore, the more refined mesh generated results closer to the experimental data, as expected.

4. CONCLUSIONS

The analysis of the velocity profiles showed that both models were able to predict the cyclone flow pattern correctly, with a rotational movement around the central axis and with an inverted W-shaped profile for axial mean velocity. Despite the similar general behavior the hybrid model obtained higher values for the mean and RMS velocities.

The analysis of the turbulent kinetic energy evidenced the concept of the used hybrid model, which uses the RSM model close to the wall, modeling more scales, and the LES in the outer flow region, making the solved turbulent kinetic energy portion greater than the modeled one.

The diferences found in the velocity profiles and in the components of turbulent kinetic energy reflected in the particle motion. Solving more turbulent scales and generating higher values of velocity, made the hybrid model to obtain collection efficiency curves closer to the experimental data than the RSM model, even for the coarser mesh.

With these analysis it is possible to conclude that the hybrid LES/RSM model proposed by the current paper is capable to realistically predict the fluid flow pattern as well as the RSM, wich is currently used in several studies of computational fluid dynamics applied to cyclones. Futhermore, analysing the particles behavior, it is possible to conclude that the hybrid model is able to predict the particles motion better than the RSM model, without the need for a more refined mesh and, consequently, an increse in the computational cost.

5. ACKNOWLEDGEMENTS

The authors would like to acknowledge the financial support from Fundação de Amparo à Pesquisa do Estado de Minas Gerais (FAPEMIG) and from Coordenação de Aperfeiçoamento de Pessoal de Nível Superior (CAPES).

6. REFERENCES

Hadžiabdic, M. and Hanjalic, K., 2020. "Elliptic-relaxation hybrid rans-les (er-hrl) for complex wall-bounded fluid and heat flows". In *Progress in rans-based scale-resolving flow simulation methods II, ERCOFTAC, bulletin 121*.

Hoffmann, A.C. and Stein, L.E., 2008. *Gas Cyclones and Swirl Tubes: Principles, Design and Operation*. Springer, 2nd edition.

Salvo, R.V., 2009. *Efeitos de modelos submalha em escoamentos em ciclones.* Master thesis, Universidade Federal de Uberlândia, Uberlândia, Brasil.

Santos, J.G.F., 2019. *Modelagem matemática e computacional de escoamentos gás-sólido em malha adaptativa dinâmica.* Master thesis, Universidade Federal de Uberlândia, Uberlândia, Brasil.

Shiller, L. and Naumann, A., 1935. "A drag coefficient correlation". *Zeitschrift des Vereins Deutscher Ingenieure*, Vol. 77, pp. 318–320.

Shukla, S.K., Shukla, P. and Ghosh, P., 2013. "The effect of modeling of velocity fluctuations on prediction of collection efficiency of cyclone separators". *Applied Mathematical Modelling*, Vol. 37, pp. 5774–5789.

Silveira Neto, A., 2001. *Turbulência nos Fluidos Aplicada*. Universidade Federal de Uberlândia.

Souza, F.J., Salvo, R.V. and Martins, D.A.M., 2012. "Large eddy simulation of the gas–particle flow in cyclone separators". *Separation and Purification Technology*, Vol. 94, pp. 61–70.

Xiang, R., Park, S. and Lee, K., 2001. "Effects of cone dimension on cyclone performance". *Journal of Aerosol Science*, Vol. 32, pp. 549–561.

7. RESPONSIBILITY NOTICE

The authors are the only responsible for the printed material included in this paper.